InAs self-assembled quantum dots as controllable scattering centers near a two-dimensional electron gas

E. Ribeiro
Laboratorium für Festkörperphysik, ETH Zürich, 8093 Zürich, Switzerland

E. Müller
Labor für Mikro- und Nanostrukturen, Paul-Scherrer Institut, 5232 Villigen, Switzerland

T. Heinzel
Laboratorium für Festkörperphysik, ETH Zürich, 8093 Zürich, Switzerland

H. Auderset
Labor für Mikro- und Nanostrukturen, Paul-Scherrer Institut, 5232 Villigen, Switzerland

K. Ensslin
Laboratorium für Festkörperphysik, ETH Zürich, 8093 Zürich, Switzerland
and Labor für Mikro- und Nanostrukturen, Paul-Scherrer Institut, 5232 Villigen, Switzerland

G. Medeiros-Ribeiro and P. M. Petroff
Materials Department, University of California, Santa Barbara, California 93106
(Received 4 February 1998)

InAs self-assembled quantum dots are grown in the vicinity of a two-dimensional electron gas. Transport experiments show a progressive reduction of the electron mobility with increasing dot density, which indicates the influence of the quantum dots on the electrical properties of the electron gas. A saturation of the mobility is observed for the highest dot density samples. Transmission electron microscopy studies confirm the existence of the dots and reveal the formation of a vertically aligned double dot. Calculations of scattering times due to repulsive potentials are in agreement with the experimental data and suggest that the self-assembled quantum dots act as controllable scattering centers that can be used to tailor the electron gas properties. [S0163-1829(98)08027-8]

INTRODUCTION

Recent developments in epitaxial techniques have permitted the *in situ* growth of high-quality defect-free quantum dots.[1–3] Due to its ~7% lattice mismatch with respect to the GaAs, InAs layers start to grow commensurate until a critical thickness is reached, when islands form spontaneously. This is the so-called Stranski-Krastanow growth mode. To achieve coherent islanding with good size uniformity the InAs epitaxy is stopped before misfit dislocations start to release the strain.[1] These randomly distributed self-assembled quantum dots (SAQD) have been extensively studied by several experimental techniques, such as photoluminescence (PL),[4–6] far-infrared spectroscopy,[7,8] capacitance spectroscopy,[7,9–11] and tunneling,[12] but little work has been done on the transport properties of SAQD located near a two-dimensional electron gas (2DEG),[13–15] despite the promising technological applications such as lasers[16,17] and optical memories.[18] Sakaki *et al.* showed that the electron mobility at 77 K is significantly reduced when the plane of SAQD gets closer to the 2DEG,[13] while Yusa and Sakaki investigated the light-dependent carrier-trapping effect of the InAs dots,[14] also at 77 K. Horigushi *et al.* studied electron transport through InAs SAQD using a split gate and measured an energy gap associated with the charging energy of the dots.[15]

In the present work we report on a systematic investigation of the transport properties of a 2DEG with embedded SAQD. In contrast to Ref. 13, we kept the position of the SAQD plane fixed relative to the 2DEG and varied the number of dots per unit area (dot density) to show that the SAQD definitely influence the transport properties of the electron gas by strongly reducing its mobility as the dot density increases. The repulsive character of the scattering potential of the charged dots is experimentally verified and calculations of scattering times result in dot densities compatible with those obtained by transmission electron microscopy (TEM).

I. EXPERIMENTAL DETAILS

Figure 1 shows a self-consistent calculation for the potential profile of the heterostructure grown for this work. After desorbing the oxides off the GaAs (001) substrate (at 650 °C), a 5000-Å GaAs buffer layer, a short-period superlattice [40×(20/20) Å AlAs/GaAs] and another 5000-Å GaAs layer were grown, at 620 °C and As pressure of 8×10^{-6} Torr. A plane of self-assembled quantum dots (shown schematically in Fig. 1 by dashed lines) was then embedded in the GaAs buffer layer 30 Å from the interface $Al_xGa_{1-x}As/GaAs$ that defines the 2DEG, near the maximum of the electronic wave function. The InAs layer was

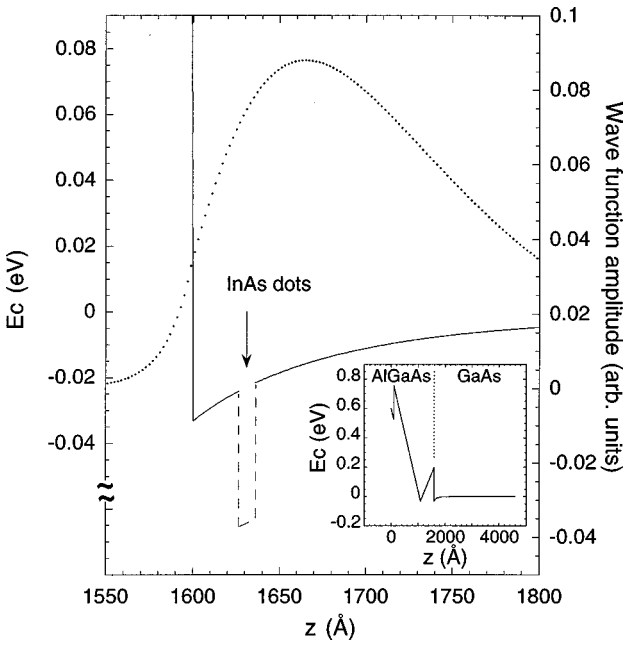

FIG. 1. Self-consistently calculated potential profile (continuous lines) and wave function (dotted curve) displayed in the region near the $Al_xGa_{1-x}As/GaAs$ interface for a heterostructure without SAQD (z is the growth direction). InAs dots contribute with a deep potential well, indicated schematically by dashed lines. The inset shows the complete structure starting from the surface ($z=0$).

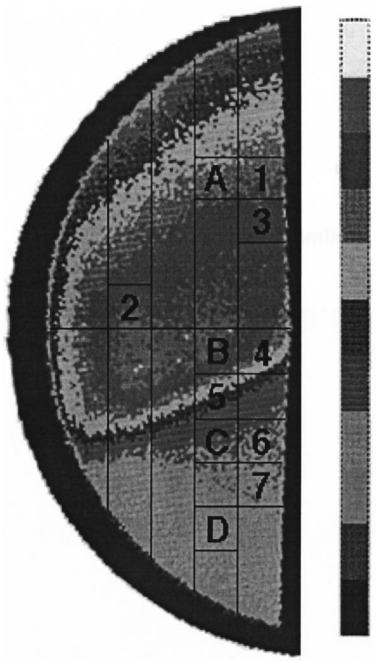

FIG. 2. Photoluminescence map of the InAs SAQD wafer integrated in the window 8000–9000 Å, around the GaAs band gap. Higher PL intensity means lower dot densities, so that a gradient (increase) in dot distribution over the wafer is achieved along the diameter from top to bottom in the figure. The dark contour around the half wafer is the sample holder backscattered light.

grown at 530 °C with a rate of 0.1 ML/s. The temperature was ramped up to the previous value while growing the remaining 30 Å of GaAs and the 1000-Å $Al_xGa_{1-x}As$ layer. A δ-doping layer within the barrier at 300 Å from the interface provides the carriers for the 2DEG. The structure was finally capped with 100 Å of GaAs. A mobility of the order of $1\,m^2/(V\,s)$ is expected due to the influence of the InAs layer.[13]

Photoluminescence (PL) spectra were taken at room temperature with the 4880-Å-line of an Ar^+ laser and a conventional photon counter detection system, the PL intensity being integrated in the window 8000–9000 Å. Low-frequency (13 Hz) transport measurements were performed at 1.7 K with an 0–8-T superconductor magnet. Magneto (ρ_{xx}) and Hall (ρ_{xy}) resistivities were measured with lock-in amplifiers using a low-signal excitation current (20–50 nA) and the front gate voltage was provided by a low-noise dc voltage source. High-resolution cross-section transmission electron microscope pictures were taken in [110] and [100] orientations with a Philips CM30ST microscope operated at 300 kV, with point-to-point resolution of 1.9 Å.

II. RESULTS AND DISCUSSION

The SAQD layer was grown without rotation of the substrate, so that a gradual variation of In concentration along a wafer diameter is achieved, the host heterostructure remaining homogeneous. This gradient of In concentration produces a gradient in the dot density. PL measurements (not shown) along the gradient line taken after the growth indicate that the SAQD recombination (~ 1.24 eV) decreases in intensity (compared to the GaAs PL) as the dot density decreases. A more complete PL map,[19] displayed in Fig. 2, shows the gradient of SAQD across the 2-in wafer. Although clearly not homogeneous in the centimeter range, TEM studies (discussed below) show that the SAQD dot density presents no significant variation within the micrometer range of the lithographic patterns used for the electrical measurements. Based on the PL map of Fig. 2, we prepared samples 1 to 7 for transport experiments and specimens A to D for TEM studies, following a trend of increasing dot density in both sets (see Fig. 2). Hall bars of 20μm width with a homogeneous Ti/Au gate evaporated on top were prepared by conventional optical lithography to study magneto and Hall resistivities. For structural characterization the set of samples A–D was prepared for cross-section TEM investigation; after a mechanical prethinning they were ion etched at an etching angle of 3° using Ar gas at 4 kV accelerating voltage.

In Fig. 3 the ρ_{xx} and ρ_{xy} spectra of samples 1 (lowest dot density) and 7 (highest dot density) are displayed for comparable carrier densities (N_s). Well-defined quantum Hall plateaus and corresponding zeros in the magnetoresistivity demonstrate the good quality of sample growth and processing. The values of ρ_{xx} at $B=0$ (see Fig. 3) directly indicate that the increasing number of dots per unit area influences the transport properties of the 2DEG by considerably lowering its mobility μ from $6.2\ m^2/(V\,s)$ [Fig. 3(a)] to $1.0\ m^2/(V\,s)$ [Fig. 3(b)]. Also the oscillations in ρ_{xx} are much less pronounced in the high dot density sample, clearly indicating that the SAQD (and not only the presence of an InAs wetting layer) actually influence the transport properties of a 2DEG. Using a gate bias to change the carrier density, a series of measurements similar to those presented in Fig. 3 were taken for all seven samples. Both carrier density and mobility were extracted from the low-field part of the

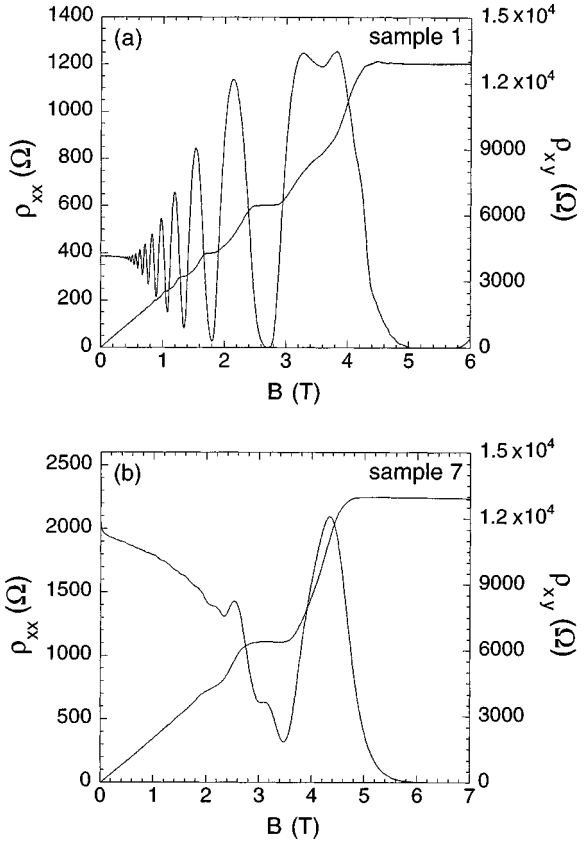

FIG. 3. ρ_{xx} and ρ_{xy} spectra for (a) the lowest and (b) the highest dot density samples taken at comparable carrier density ($\sim 2.6 \times 10^{15}$ m^{-2} and $\sim 3.1 \times 10^{15}$ m^{-2}, respectively). The influence of the SAQD on the transport properties is clearly seen in the strong reduction of the mobility, from 6.2 m^2/(V s) in sample 1 to 1.0 m^2/(V s) in sample 7.

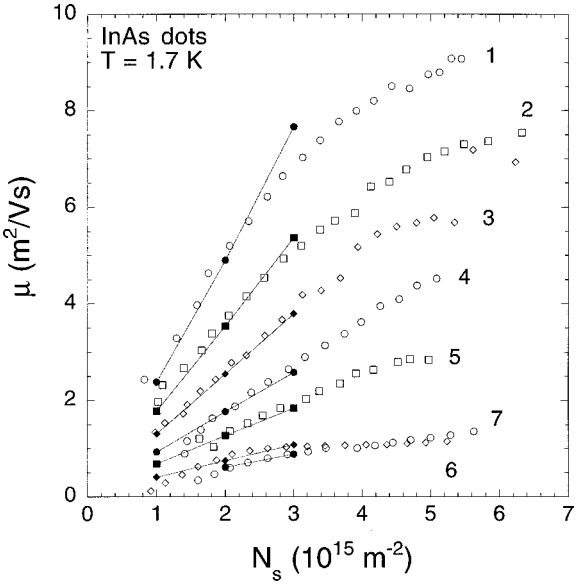

FIG. 4. Mobility as a function of the carrier density for samples 1 to 7 (open symbols). The influence of the number of scattering centers (SAQD) is clearly seen by the decrease of the 2DEG mobility as the dot density increases (at a given N_s). For high density samples (6 and 7) the mobility seems to saturate. Closed symbols are the mobilities obtained by scattering time calculations as described in the text. Lines are guides to the eye.

spectra and the μ versus N_s curves are shown in Fig. 4 (open symbols). For a given N_s, the 2DEG mobility progressively decreases as the SAQD density increases (from sample 1 to 7), as is expected if one supposes that the SAQD act as the dominant scattering mechanism in these samples. Another feature present in Fig. 4 is the apparent mobility saturation for samples 6 and 7 (highest dot densities) as a function of N_s: this might indicate that the average separation among dots is comparable to the two-dimensional screening length of the electrons so that the scattering centers cannot be effectively screened any further; the mobility, thus, would change very little with increasing carrier density, consistent with SAQD acting as scattering centers. Since the screening length λ_s in two dimensions is constant,[20] one can estimate a dot density n_{sl} corresponding to the picture described above. Considering the dots as rigid disk-shaped scattering centers, a dot density of $n_{sl} = 4.7 \times 10^{10}$ cm^{-2} would give the desired average separation of $\lambda_s = 320$ Å. This number is consistent with typical dot densities determined by atomic force microscopy for InAs SAQD samples,[3] giving support to our proposition. Due to the actual long-range character of the Coulomb potential, this number must be seen as an upper limit.

To shed more light on this issue we studied the behavior of the Hall resistivity. It is known that the centers of the quantized plateaus in ρ_{xy} deviate from the classical free-electron result $\rho_{xy}^c = B/eN_s$ in the presence of charged impurities.[21] In particular, repulsive scattering potentials shift the plateaus to higher magnetic fields (smaller filling factors).[21] Figure 5 shows the Hall resistivities for $N_s = 1.6 \times 10^{15}$ m^{-2}. The magnetic field axis was redefined so that $B_{\text{eff}} = 0$ represents the intersection between the classical value and the measured Hall plateaus for each sample. A progressive shift of the plateaus to higher magnetic fields is observed, coherent with the expected repulsive character of the charged SAQD. In addition, samples 6 and 7 have a ρ_{xy} plateau that closely resembles the data of Haug *et al.*[21] for a Be δ doping with $n_i = (3D)4.0 \times 10^{10}$ cm^{-2}, which can also be taken as an upper limit for our samples because the SAQD may contain more than one electron per dot.

With this in mind, we modeled our samples as a usual 2DEG ($Al_xGa_{1-x}As/GaAs$ interface and remote doping layer in the barrier) with a plane of repulsive scattering centers placed at the SAQD nominal position. Using the Stern-Howard model[22,20,23] one can write the inverse scattering time as[23]

$$\frac{1}{\tau_i} = \frac{1}{2\pi\hbar\varepsilon_F} \int_0^{2k_F} dq \, \frac{q^2}{\sqrt{4k_F^2 - q^2}} \, \frac{\langle |U_i(\mathbf{q})|^2 \rangle}{\epsilon(q)^2}, \qquad (1)$$

where $\hbar$ is the Planck's constant, $\varepsilon_F(k_F)$ is the Fermi energy (wave number), q is the scattering wave number, and $\epsilon(q)$ is the dielectric function of the electron gas.[20,23] A two-dimensional sheet of random impurities is described by the potential

$$\langle |U_i(\mathbf{q})|^2 \rangle = n_i \left(\frac{2\pi e^2}{\kappa} \frac{1}{q} \right)^2 F(q, z_i)^2, \qquad (2)$$

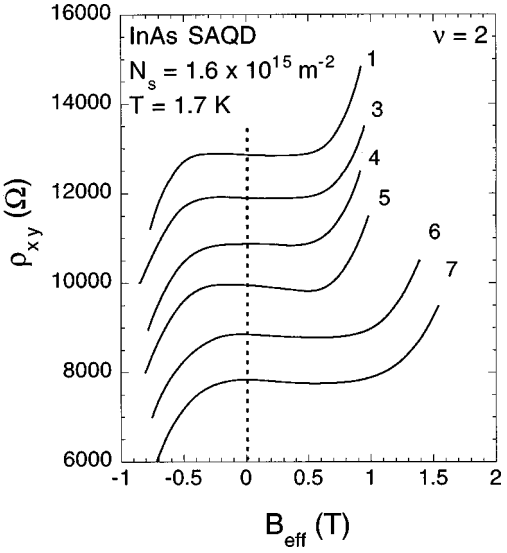

FIG. 5. Hall resistivity as a function of magnetic field for the samples taken along the wafer diameter, displayed in the region around filling factor $\nu=2$. The effective magnetic field is defined in a way that at $B_{\rm eff}=0$ one finds the crossing point between the experimental data and the extrapolation of the classical behavior for the Hall resistivity at low magnetic fields. The center of the plateaus deviates from $B_{\rm eff}=0$ to higher magnetic fields, indicating the presence of repulsive scattering potentials in the samples. The trend of increasing deviation from top to bottom agrees with the increasing dot density already determined. The ρ_{xy} spectrum of sample 2 was not displayed because of lack of processing quality.

where n_i is the impurity density, e is the electronic charge, κ is the static dielectric constant of the semiconductor, and $F(q,z_i)$ is a form factor that takes into account the finite extension of the 2DEG and the distance z_i between the impurity plane and the interface.[20] The various contributions to the scattering process add according to Matthiessen's rule. In our case we used a remote doping concentration of 1.17×10^{12} cm^{-2} (as in the self-consistent calculations of Fig. 1) and a homogeneous background doping to describe the presence of a InAs wetting layer. This bulk doping concentration n_B was set to 7.6×10^{15} cm^{-3} to reproduce the mobility of sample 1, assumed from here on to have no SAQD. With these two parameters kept fixed, we introduced the repulsive scattering plane with the impurity density $n_{\rm SAQD}$ as a free parameter to fit the data. The results for a SAQD containing 2 electrons are shown in Fig. 4 (closed symbols) for all the samples. The $n_{\rm SAQD}$ obtained are listed in Table I and are consistent with those experimentally found in the literature[3] and also with the n_{sl} suggested above for samples 6 and 7.

Figure 6 shows TEM micrographs of specimens *A*, *B*, and *C* (see Fig. 2), representing three different growth areas along the wafer, depending on the amount of InAs that had been deposited on the respective positions. In Fig. 6(a) (sample *A*), a single row of bright points between the two GaAs layers indicates the presence of a very thin interfacial layer between the GaAs buffer and the 30-Å-thick GaAs layer. It is thinner than 4 ML, being consistent with the expected InAs wetting layer 1–2 ML thick.[1,2] For sample *B* (coming from a region of the wafer where more InAs had been deposited), a faint contrast of a noncontinuous layer is observed, its thickness being in the range of 4–6 ML [see Fig. 6(b)]. In this area of the specimen the maximum thickness for a purely two-dimensional growth mode of InAs is exceeded. The formation of the dots has therefore started although it is not yet very pronounced. In the specimens containing more indium (samples *C* and *D*) a large number of dots is clearly seen. Most of them, however, have a rather complicated, sandwichlike structure. A dark contrast of 20–25 nm lateral extension and about 8 ML thickness is visible adjacent to the lower GaAs layer [Fig. 6(c)]. After a brighter region of nearly the same thickness, a second dark layer is observed atop. Such a contrast was found everywhere within the electron-transparent area of the high-density samples, independent of the local specimen thickness. A bending of the sample due to strain effects, as is commonly observed close to the specimen edge due to foil effects, can therefore be ruled out as an explanation for this contrast. Measuring the interplanar distances within the different regions on high-resolution micrographs taken along the [100] direction revealed that in the lower dark layer the vertical lattice parameter was in the range of 3.5–4.0% larger than that of GaAs. In the upper dark disk region, the lattice parameter was always equal to or larger (between 1–4%) than that of GaAs, while between these two dark regions $a\sim a_{\rm GaAs}$ was measured in all cases. It can therefore be supposed that in a first stage a simple dot of 20–25 nm diameter, about 6 ML thickness, and a vertical lattice parameter $a_{\rm SAQD}$ of nearly $a_{\rm SAQD}\sim1.04a_{\rm GaAs}$ is formed. In the high dot density areas, the excess of In floats on top of the dot towards the GaAs/$Al_xGa_{1-x}As$ interface, where it forms a second In-rich layer as soon as the $Al_xGa_{1-x}As$ is deposited. Its vertical lattice parameter varies (according to the amount of In) between that of GaAs and that of the lower dot. This is consistent with PL measurements across the wafer, where a second peak is present for the highest dot densities, its inten-

TABLE I. Comparison between the dot densities obtained experimentally and theoretically. $n_{\rm SAQD}$ are the results of the Stern-Howard scattering time model using a remote barrier doping layer (carriers) and a residual bulk impurity concentration (wetting layer) for describing the 2DEG mobility without SAQD (see text), and a plane of doubly charged repulsive scattering centers to describe the dots. $n_{\rm TEM}$ is an average value obtained from TEM studies. These numbers are in reasonable agreement with the upper limits estimated from the μ vs N_s curves (4.7×10^{10} cm^{-2}) and the ρ_{xy} plateau analysis (4.0×10^{10} cm^{-2}).

Transport		TEM	
Sample	$n_{\rm SAQD}$ (cm^{-2})	Specimen	$n_{\rm TEM}$ (cm^{-2})
1	0	*A*	[a]
2	5.5×10^{9}		
3	1.3×10^{10}		
4	2.5×10^{10}	*B*	[b]
5	4.1×10^{10}		
6	7.9×10^{10}	*C*	2.5×10^{10}
7	1.0×10^{11}		
		D	3.0×10^{10}

[a]No SAQD observable experimentally.
[b]Too few SAQD to obtain reasonable error bars in the statistics.

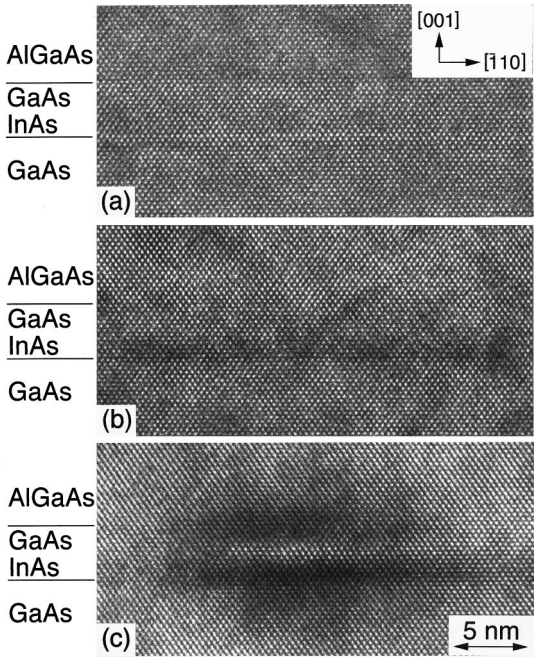

FIG. 6. High-resolution cross-section TEM micrographs taken in the [110] orientation: (a) specimen *A*, showing a brighter row corresponding to the InAs wetting layer and no dots; (b) specimen *B*, where noncontinuous In-rich layers are observed with a faint contrast, indicating the formation of SAQD; (c) specimen *C*, showing a sandwichlike InAs dot formed by a SAQD in the nominal position and on top of it an InAs-rich layer that has segregated towards the $Al_xGa_{1-x}As$/GaAs interface. The nominal component layers are indicated on the left side of the pictures. Growth direction [001] (top) as well as scale (bottom) are valid for all three micrographs.

sity completely vanishing when lower dot densities are reached. The formation of the second dot may also be related to the results of Garcia *et al.*,[24] where they observe a crater-like depression in the middle of the partially covered dots after a GaAs coverage of 20 Å, very similar to that of our samples (30 Å). As a possible explanation, we suggest that the excess In floating on the surface of the covered dots (in the high dot density areas of our wafer) would be confined to these depressions by the $Al_xGa_{1-x}As$ layer, giving rise to the observed vertical self-alignment [see Fig. 6(c)]. An attempt was made to estimate the dot density in the different specimens from the TEM micrographs. The thickness variation of the cross-sectional TEM samples (up to 4μm wide) was calculated from the respective thickness fringes. The dots could not be counted in sample *B* because their contrast was too weak. In samples *C* and *D* densities of $(2.5\pm1.0)\times10^{10}$ cm^{-2} and $(3.0\pm1.0)\times10^{10}$ cm^{-2} were found, respectively. This is in good agreement with the numbers estimated from transport measurements and scattering time calculations (see Table I).

The TEM results support the assumption made in the scattering time calculation, that sample 1 should nominally contain no quantum dots. The observation of the double-dot structure would allow us to include a second layer of scattering centers in the model, reducing the n_{SAQD} of Table I to values closer to those determined by TEM (and below the two upper limits discussed above). The scattering properties of the SAQD are only slightly changed (about 10%) if the position of the dots is moved from the intended position (30 Å from the interface) to the interface itself. In both cases the electron wave function overlaps with the position of the dots. Once the number of electrons in the SAQD is also a free parameter, a suitable combination of both could bring TEM results and calculations into coincidence; however, we have already reached an overall agreement for the dot density within the same order of magnitude for data coming from completely different experimental sources. We also note that the double dot appears in a region of the original wafer in which the 2DEG mobility is seen to saturate as a function of the carrier density, indicating a possible connection between the two observations.

In summary, the good agreement between calculated dot densities and those obtained from transport and TEM data is a clear and quantitative evidence of the influence of self-assembled quantum dots on the properties of a 2DEG. The dots can be seen as randomly distributed repulsive scattering centers that reduce the electron gas mobility as the dot density increases, up to a limit where the electrons are unable to screen the charged dots any further, leading to a saturation in the mobility. The SAQD can be used as controllable scattering centers to tailor the electrical properties of a 2DEG.

ACKNOWLEDGMENTS

We would like to thank Dr. T. Ihn for fruitful discussions. One of us (E.R.) gratefully acknowledges financial support from Fundação do Amparo à Pesquisa do Estado de São Paulo.

[1] D. Leonard, M. Krishnamurthy, C. M. Reaves, S. P. Denbaars, and P. M. Petroff, Appl. Phys. Lett. **63**, 3203 (1993).

[2] J. M. Moison, F. Houzay, F. Barthe, L. Leprince, E. André, and O. Vatel, Appl. Phys. Lett. **64**, 196 (1994).

[3] D. Leonard, K. Pond, and P. M. Petroff, Phys. Rev. B **50**, 11 687 (1994).

[4] S. Fafard, D. Leonard, J. L. Merz, and P. M. Petroff, Appl. Phys. Lett. **65**, 1388 (1994).

[5] J.-Y. Marzin, J.-M. Gérard, A. Izraël, D. Barrier, and G. Bastard, Phys. Rev. Lett. **73**, 716 (1994).

[6] R. Leon, P. M. Petroff, D. Leonard, and S. Fafard, Science **267**, 1966 (1995).

[7] H. Drexler, D. Leonard, W. Hansen, J. P. Kotthaus, and P. M. Petroff, Phys. Rev. Lett. **73**, 2252 (1994).

[8] M. Fricke, A. Lorke, J. P. Kotthaus, G. Medeiros-Ribeiro, and P. M. Petroff, Europhys. Lett. **36**, 197 (1996).

[9] G. Medeiros-Ribeiro, D. Leonard, and P. M. Petroff, Appl. Phys. Lett. **66**, 1767 (1995).

[10] G. Medeiros-Ribeiro, F. G. Pikus, P. M. Petroff, and A. L. Efros, Phys. Rev. B **55**, 1568 (1997).

[11] B. T. Miller, W. Hansen, S. Manus, R. J. Luyken, A. Lorke, J. P. Kotthaus, S. Huant, G. Medeiros-Ribeiro, and P. M. Petroff, Phys. Rev. B **56**, 6764 (1997).
[12] I. E. Itskevich, T. Ihn, A. Thornton, M. Henini, H. A. Carmona, L. Eaves, P. C. Main, D. K. Maude, and J.-C. Portal, Jpn. J. Appl. Phys., Part 1 **36**, 4073 (1997).
[13] H. Sakaki, G. Yusa, T. Someya, Y. Ohno, T. Noda, H. Akiyama, Y. Kadoya, and H. Noge, Appl. Phys. Lett. **67**, 3444 (1995).
[14] G. Yusa and H. Sakaki, Appl. Phys. Lett. **70**, 345 (1997).
[15] N. Horiguchi, T. Futatsugi, Y. Nakata, and N. Yokoyama, Appl. Phys. Lett. **70**, 2294 (1997).
[16] H. Saito, K. Nishi, I. Ogura, S. Sugou, and Y. Sugimoto, Appl. Phys. Lett. **69**, 3140 (1996).
[17] S. Fafard, K. Hinzer, S. Raymond, M. Dion, J. McCaffrey, Y. Feng, and S. Charbonneau, Science **274**, 1350 (1996).
[18] K. Imamura, Y. Sugiyama, Y. Nakata, S. Muto, and N. Yokoyama, Jpn. J. Appl. Phys., Part 2 **34**, L1445 (1995).
[19] Due to experimental limitations only the GaAs contribution for the PL was integrated (the SAQD PL structures are located at $\sim$10000 Å). The dot density is higher where the GaAs PL is lower. A color printout is available upon request.
[20] T. Ando, A. B. Fowler, and F. Stern, Rev. Mod. Phys. **54**, 437 (1982).
[21] R. J. Haug, R. R. Gerhardts, K. v. Klitzing, and K. Ploog, Phys. Rev. Lett. **59**, 1349 (1987).
[22] F. Stern and W. E. Howard, Phys. Rev. **163**, 816 (1967).
[23] A. Gold, Phys. Rev. B **38**, 10 798 (1988).
[24] J. M. García, G. Medeiros-Ribeiro, K. Schmidt, T. Ngo, J. L. Feng, A. Lorke, J. Kotthaus, and P. M. Petroff, Appl. Phys. Lett. **71**, 2014 (1997).